Macromolecular Rapid Communications
www.mrc-journal.de

A Useful Method for Preparing Mixed Brush Polymer Grafted Nanoparticles by Polymerizing Block Copolymers from Surfaces with Reversed Monomer Addition Sequence

*Yang Zheng, Yucheng Huang, and Brian C. Benicewicz**

The preparation of well-defined block copolymers using controlled radical polymerization depends on the proper order of monomer addition. The reversed order of monomer addition results in a mixture of block copolymer and homopolymer and thus has typically been avoided. In this paper, the low blocking efficiency of reversed monomer addition order is utilized in combination with surface initiated reversible addition–fragmentation chain-transfer polymerization to establish a facile procedure toward mixed polymer brush grafted nanoparticles SiO_2-*g*-(PS (polystyrene), PS-*b*-PMAA (polymethacrylic acid)). The SiO_2-*g*-(PS, PS-*b*-PMAA) nanoparticles are analyzed by gel permeation chromatography deconvolution, and the fraction of each polymer component is calculated. Additionally, the SiO_2-*g*-(PS, PS-*b*-PMAA) are amphiphilic in nature and show unique self-assembly behavior in water.

1. Introduction

It is now well accepted that the order of monomer addition is pivotal in the preparation of well-defined block copolymers using controlled radical polymerization.[1,2] Because of the better leaving group ability, monomers that produce tertiary propagating radicals (e.g., methacrylates) should be polymerized prior to those that produce secondary propagating radicals (e.g., acrylates and styrene). For example, the chain extension of styrene from polymethyl methacrylate (PMMA) macroinitiator is considered the "right sequence" toward well-defined PMMA-*b*-PS (polystyrene). In contrast, the reversed monomer addition sequence leads to mixed products of homopolymer and block copolymer because of the slow initiation of the macroinitiators. Thus, only some of the macroinitiators can be successfully chain extended which leads to the mixture of homopolymers and block copolymers.[3] This reversed monomer addition order sometimes called the "wrong sequence" has always been avoided when making block copolymers using controlled radical polymerization methods. Indeed, the product as a copolymer/homopolymer mixture is not of interest for most research and applications. However, we envision that this scenario could be synthetically and practically attractive when the macroinitiators are anchored onto the surface of a substrate or nanoparticles. When the polymer chains are grafted on a substrate or particle surfaces and surface-initiated polymerizations are performed, it is possible that we could advantageously utilize the outcome of this "wrong sequence" to prepare mixed brush polymer grafted nanoparticles in a simplified process.

Nanoparticles with two different populations of polymer brushes have been a topic of increasing importance in ligand engineering of polymer nanocomposites.[4–8] Recent advances in surface initiated (SI) polymerization creates the possibility to fabricate such composite materials with good interfacial properties via control of the graft density, molecular weight, and chemistry of the grafted polymers. However, the preparation procedures are typically time consuming and involve multiple steps. For example, the preparation of bimodal polymer grafted nanoparticles using surface-initiated reversible addition–fragmentation chain-transfer (SI-RAFT) polymerization include at least five steps: (1) polymerization of first brush, (2) chain end RAFT agent cleavage, (3) aminosilane attachment, (4) second RAFT attachment, and (5) polymerization of second brush. Each step is accompanied by at least two washings and precipitations, making the whole process relatively time consuming.[6,9,10] Similarly, the preparation of such materials using SI atom-transfer radical-polymerization includes multiple steps to partially deactivate the chain end of the first population of polymer brushes.[8]

In this work, we explored surface initiated RAFT polymerization using reversed monomer addition sequence as a simple two step method of preparing mixed brush grafted nanoparticles consisting of a shorter polystyrene homopolymer brush and a longer polystyrene-*b*-polymetharcylic acid brush. Moreover, these amphiphilic nanoparticles showed unique self-assembly behavior in water, forming nanoparticle clusters with controlled aggregation number.

2. Results and Discussion

2.1. Synthesis of SiO_2-*g*-(PS, PS-*b*-PMAA) Using Reversed Monomer Addition Sequence

A 4-cyanopentanoic acid dithiobenzoate (CPDB) RAFT agent was initially attached to 15 nm silica nanoparticles, as reported

Dr. Y. Zheng, Y. Huang, Prof. B. C. Benicewicz
Department of Chemistry and Biochemistry
University of South Carolina
Columbia, SC 29208, USA
E-mail: benice@sc.edu

The ORCID identification number(s) for the author(s) of this article can be found under https://doi.org/10.1002/marc.201700300.

DOI: 10.1002/marc.201700300

 © 2017 WILEY-VCH Verlag GmbH & Co. KGaA, Weinheim

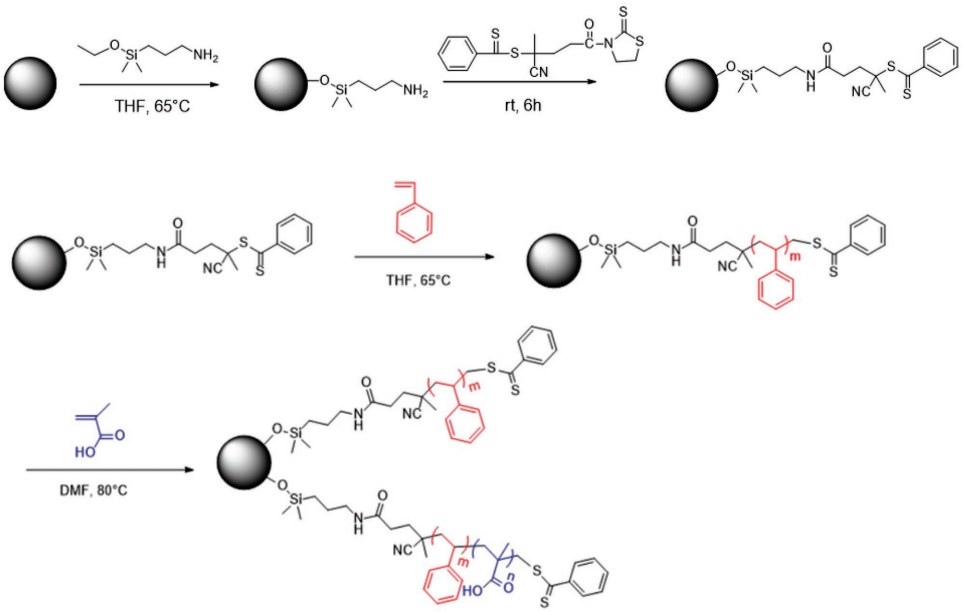

Figure 1. Synthetic scheme of SiO_2-*g*-(PS, PS-*b*-PMAA) using reversed monomer addition sequence.

previously.[6] The graft density was determined by UV–vis analysis to be 0.27 ch nm^{-2} (Figure S1, Supporting Information). To perform the polymerization in reversed sequence, we polymerized styrene from nanoparticle surfaces in the first step, followed by the chain extension of the macroinitiator with methacrylic acid (**Figure 1**). The initial SI-RAFT of PS was performed in tetrahydrofuran (THF) for 11 h at 65 °C. From a small sample, the grafted polymers were cleaved from the silica particle surface and characterized using gel permeation chromatography (GPC) (21 kDa, $Đ = 1.1$). The PS grafted nanoparticles were purified, redispersed in *N*,*N*-dimethylformamide (DMF), and chain extended with methacrylic acid. The polymerization of MAA was conducted at 80 °C at various times. The resulting polymer grafted particles were treated with hydrofluoric acid (HF) to etch the silica, and the polymers were subjected to GPC analysis (**Table 1**).

Figure 2 shows a typical GPC curve of PS-*b*-PMAA (polymethacrylic acid) copolymer cleaved from the nanoparticle surfaces. It should be noted that the PS-*b*-PMAA was treated with trimethylsilyldiazomethane to convert the carboxylic groups of the PS-*b*-PMMA to methyl esters before GPC injection to improve the compatibility between the polymer and the THF phase GPC (see Figure S2, Supporting Information, for details). The curves were analyzed using a deconvolution method with an Origin peak analyzer. Further calculations based on mathematical deconvolution of the GPC peaks provided a multipeak fitting for all polymer peaks. The weight fraction and mole fraction of each component was then calculated based on M_n values from GPC and adjusted by the d*n*/d*c* values of each component (see the Supporting Information for details). This GPC deconvolution method has been used by Wooley and co-workers and Howdle and co-workers as a reliable method for calculating block efficiency.[11,12]

The results show that the block copolymer GPC curves could be separated into three peaks. The first peak (≈21 kDa) appeared at the exact position as the PS macroinitiator and thus was ascribed to the PS homopolymer which did not participate in the chain extension reaction. This inactive polymer was the major component of the grafted polymers. The second peak (≈43 kDa) had twice the molecular weight of the PS homopolymer and its position did not change during the subsequent polymerizations. This indicated the presence of dead PS chains likely formed by radical recombination during the addition of 2.2′-azobisisobutyronitrile (AIBN) at the start of the chain extension or second polymerization step. The third peak had the largest molecular weight. Furthermore, the molecular weight as well as its mole fraction increased during polymerization, indicating the formation of block copolymer. At 20% monomer

Table 1. Characteristics of grafted PS-*b*-PMAA synthesized at different conversions.

Entry	Time [h]	Conversion [%]	Peak 1 M_n [kDa]	Peak 1 mole percent [%]	Peak 1 volume percent [%]	Peak 2 M_n [kDa]	Peak 2 mole percent [%]	Peak 2 volume percent [%]	Peak 3 M_n [kDa]	Peak 3 mole percent [%]	Peak 3 volume percent [%]
0	0	0	20	100							
1	2	7	21	84.8	62.7	43	8.4	12.7	104	6.7	24.5
2	4	16	20	82.9	53.8	43	8.0	10.7	126	9.1	35.5
3	7	20	21	80.6	48.2	43	8.5	10.5	132	10.9	41.3

© 2017 WILEY-VCH Verlag GmbH & Co. KGaA, Weinheim

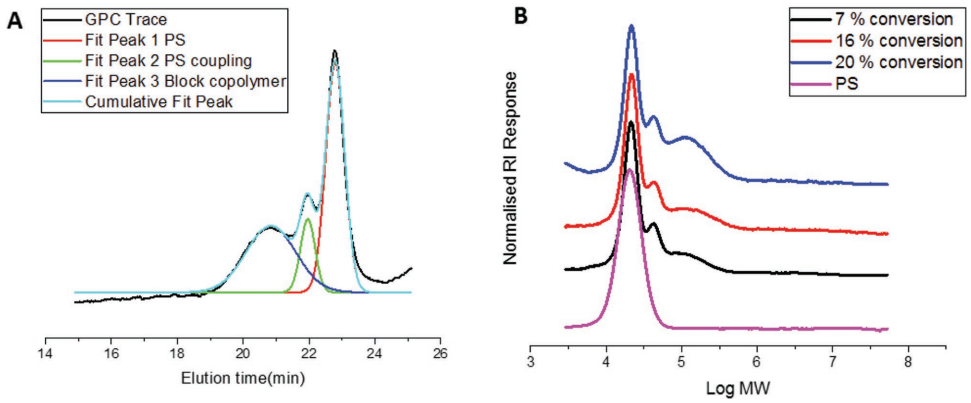

Figure 2. A) An example (Entry 3) of a typical GPC curve and fitted peaks for cleaved PS-*b*-PMAA copolymer. B) Stacked GPC traces of PS-*b*-PMAA copolymers synthesized by polymerization of MAA from surface anchored PS macroinitiator.

conversion, ≈80% of the PS macroinitiators remained "unreacted" and 8.5% of the PS chains underwent coupling thus forming PS homopolymer with double the molecular weight as the unreacted chains. Finally, 10.9% of the PS chains successfully chain extended with MAA forming block copolymers. Compared with literature data of block copolymerizations crossing from secondary radicals to tertiary radicals,[3] the block efficiency was relatively low. However, the peak ascribed to homopolymer coupling was not observed in the free solution polymerization. Here, we consider the differences between grafting-from polymerization and free solution polymerization. In the case of grafting-from polymerization, the PS macroinitiators were in close proximity as their motion was restricted by tethering onto the nanoparticle surface. Therefore, due to the slow initiation process and inefficient chain extension, the radicals on the particle surface had greater possibility to undergo termination by combination prior to polymerization. In order to demonstrate that this radical coupling occurred within each nanoparticle instead of inter-particle crosslinking, another polymerization was conducted under diluted conditions. The radical coupling peak was observed without a change in mole fraction.

2.2. Self-Assembly Behavior of SiO_2-*g*-(PS, PS-*b*-PMAA)

The self-assembly of grafted nanoparticles has been a topic of recent interest to us, thus we studied the self-assembly behavior of these (PS, PS-*b*-PMAA) grafted nanoparticles in aqueous solution.

Self-assembly was induced by the solvent switching method. Typically, PS-*b*-PMAA grafted nanoparticles were purified and dispersed in DMF, a good solvent for all components, and then water was introduced dropwise to induce the self-assembly. The solution changed from transparent to translucent, indicating the formation of nanoassemblies. The morphology of the assemblies was characterized with transmission electron microscopy (TEM) to be solid sphere aggregates. As discussed earlier, the SiO_2-*g*-(PS, PS-*b*-PMAA) nanoparticles have bimodal structures that not only change in chain length of PMAA during the polymerization but also change slightly in the portion of block copolymer. To facilitate comparisons between samples, in this section, we prepared a series of SiO_2-*g*-(PS_{396}, PS_{396}-*b*-$PMAA_x$) nanoparticles with the same PS homobrush chain length but different PS_{396}-*b*-$PMAA_x$ lengths. The subscripts denote the number of repeating units calculated from ^{1}H NMR and assumes 10% block copolymer fraction in all cases.

For the experiment using SiO_2-*g*-(PS_{396}, PS_{396}-*b*-$PMAA_{1660}$) the average size of the spheres was ≈80 nm, which was slightly less than the value measured by dynamic light scattering (DLS) (**Figure 3**A–D). The difference in size is not surprising since DLS measures hydrodynamic size including the size of extended polymer brushes and associated water molecules. Each sphere aggregate was composed of tens of smaller spherical silica nanoparticles that showed as darker contrast under TEM. We use the number ratio between PS and PMAA calculated from NMR to represent the difference of hydrophobic/hydrophilic ratio between each sample. The self-assemble structures obtained here (solid spheres) has rarely been reported, probably due to the unique surface polymer structure. The self-assembly mechanism is illustrated in Figure 3J. We believe that during water addition, the PS segments, including both homopolymer brushes and PS polymer loops formed by radical coupling collapsed and were kinetically frozen, forming the hydrophobic cores that were stabilized by PMAA segments as corona. The mole fraction between each polymer component calculated in the previous section is a statistical average value and we believe that the exact hydrophilic/hydrophobic polymer ratio on each nanoparticle differs slightly. Thus, the particles with smaller hydrophilic/hydrophobic ratio collapsed more readily and stayed in the center of the assemblies, and because of the high molecular weight of PMAA segments, the hydrophilic PMAA chains could still stretch through the aggregates and reach the surface. On the other hand, particles with larger hydrophilic/hydrophobic ratio would preferably stay near the surface of the aggregates, to better stabilize the nanoparticle clusters.

The size of aggregates as well as the aggregation number could be controlled by manipulating the hydrophilic/hydrophobic ratio of the nanoparticles. We studied the assembled structures of a series of samples with the same chain length

© 2017 WILEY-VCH Verlag GmbH & Co. KGaA, Weinheim

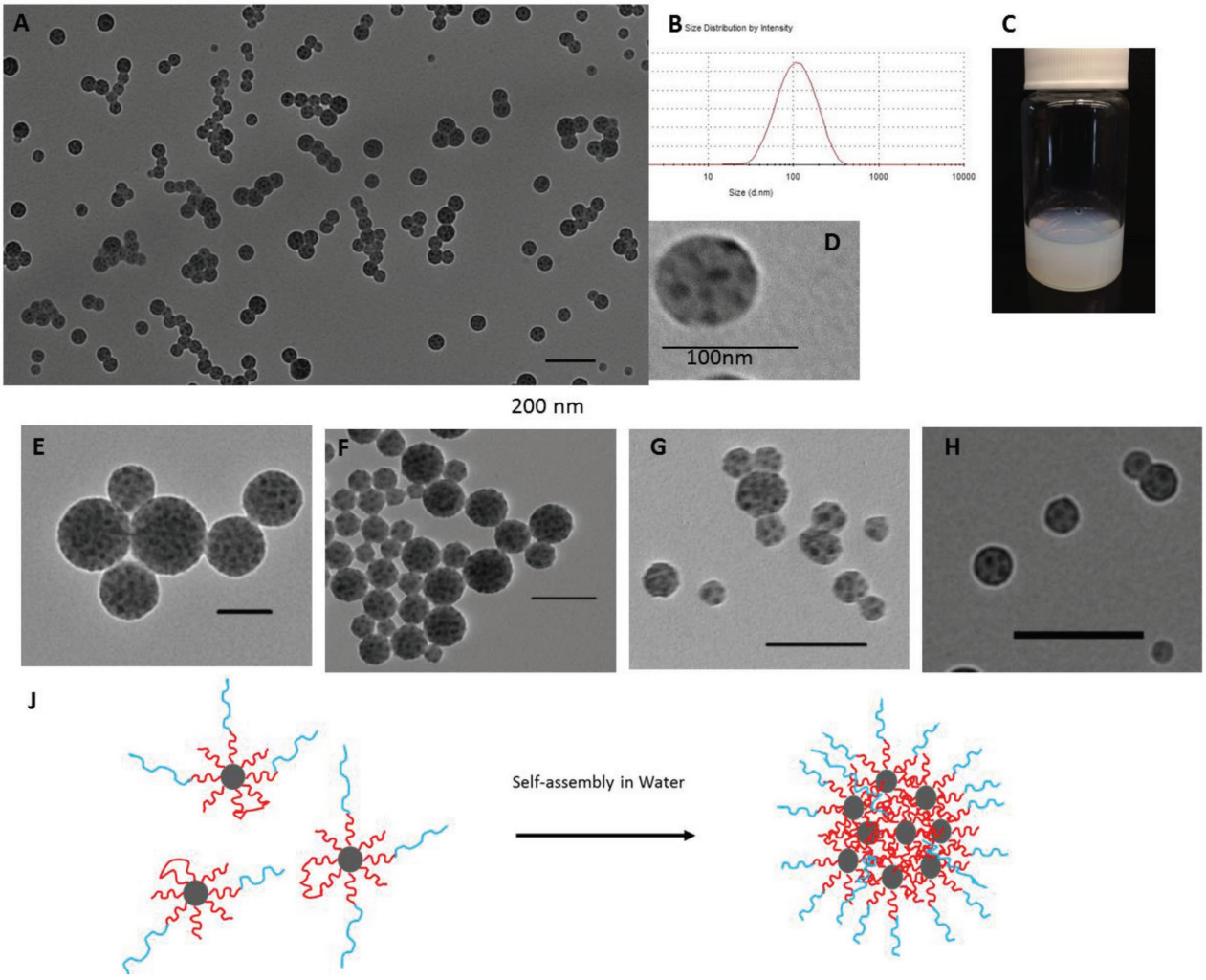

Figure 3. A–D) TEM, DLS, and visual appearance of assemblies prepared from SiO_2-*g*-(PS_{396}, PS_{396}-*b*-$PMAA_{1660}$) nanoparticles. E–H) Comparison of assembled nanospheres with different PS/PMAA ratios. Scale bars: 200 nm. E) SiO_2-*g*-(PS_{396}, PS_{396}-*b*-$PMAA_{350}$), F) SiO_2-*g*-(PS_{396}, PS_{396}-*b*-$PMAA_{500}$), G) SiO_2-*g*-(PS_{396}, PS_{396}-*b*-$PMAA_{1000}$), H) SiO_2-*g*-(PS_{396}, PS_{396}-*b*-$PMAA_{1660}$), and J) proposed self-assembly mechanism.

of the PS block but different lengths of the PMAA block (Figure 3E–H). It was clear that decreasing of size of the PMAA block produced an increase of the aggregation number. The spherical aggregates from SiO_2-*g*-(PS_{396}, PS_{396}-*b*-$PMAA_{350}$) nanoparticles consisted of tens-to-hundreds of primary silica nanoparticles (Figure 3E), while the aggregates from SiO_2-*g*-(PS_{396}, PS_{396}-*b*-$PMAA_{1660}$) consisted of only a few (<10) primary silica nanoparticles (Figure 3H).

The size of the aggregates as well as the aggregation number could also be controlled by adjusting the initial concentration of the solution using the identical sample. We prepared a series of solutions with different initial concentrations using the same SiO_2-*g*-(PS_{396}, PS_{396}-*b*-$PMAA_{1660}$) nanoparticle sample. As shown in Figure S3 in the Supporting Information, the size of the aggregates increased with increasing concentration of the initial solution. At higher concentration (50 mg mL^{-1}), the aggregate size increased to ≈150 nm while at low concentration (1 mg mL^{-1}), the degree of aggregation was very low, and the particles were mostly singly dispersed.

3. Experimental Section

3.1. Materials

Styrene (TCI, 97%) and methacrylic acid (Acros, 96%) were passed through a basic aluminum column to remove inhibitors before use. AIBN was purified by recrystallization from methanol and dissolved in ethanol to make 10×10^{-3} M solution. All other reagents were used as received.

3.2. Synthesis of PS Grafted Silica Nanoparticles

CPDB anchored 15 nm silica nanoparticles were prepared according to the literature.[1] A solution of styrene (7.96 g), AIBN (255 µL of 10×10^{-3} M solution in methanol), CPDB-anchored silica nanoparticles (0.4, 63.8 µmol g^{-1}), and THF (8 mL) was prepared in a Schlenk tube. The mixture was degassed by three freeze–pump–thaw cycles, backfilled with nitrogen, and then placed in an oil bath at 65 °C for 11 h. The polymerization

© 2017 WILEY-VCH Verlag GmbH & Co. KGaA, Weinheim

solution was quenched in an ice bath and poured into 1:1 mixture of hexane to precipitate the SiO_2-*g*-PS nanoparticles. The SiO_2-*g*-PS nanoparticles were redispersed in THF and precipitated two more times to remove excess monomers and initiators. The purified SiO_2-*g*-PS nanoparticles were dispersed in DMF for the next reaction step (Figure S4, Supporting Information).

3.3. Synthesis of SiO_2-*g*-(PS, PS-*b*-PMAA) Nanoparticles

SiO_2-*g*-PS nanoparticles (0.2 g), methacrylic acid (0.975 g), AIBN (134 µL of 10×10^{-3} M solution in ethanol), and DMF (10 mL) were mixed together and added to a Schlenk flask equipped with a rubber stopper. The mixture was degassed by three freeze–pump–thaw cycles, backfilled with nitrogen and then placed in an oil bath of 80 °C. Aliquots of the reaction solution were withdrawn from the flask periodically after the start of the polymerization. NMR (Figure S5, Supporting Information) showed the chain extension of the original PS chains. TEM (Figure S6, Supporting Information) showed that the particles were individually dispersed in good solvents such as DMF. Grafted polymer chains were cleaved from silica nanoparticles by reacting with excess amount of HF.

3.4. Preparation of Self-Assembled Nanoparticle Clusters

The SiO_2-*g*-(PS, PS-*b*-PMAA) nanoparticles were dispersed in DMF at predetermined concentration. Deionized water was added at a rate of 0.02 mL s^{-1} with vigorous stirring. Subsequently, the solution was dialyzed against deionized water over night to remove the organic solvents.

3.5. Methylation of SiO_2-*g*-(PS, PS-*b*-PMAA) Nanoparticles

SiO_2-*g*-PS-*b*-PMAA nanoparticles (≈20 mg) were dissolved in 10 mL DMF. An excess of the yellow solution of trimethylsilyldiazomethane was added dropwise into the nanoparticle solution at room temperature (RT). After complete addition, the solution was stirred for 3 h at RT. Approximately 10% by volume of methanol was added to enhance the conversion of the methylation. The excess trimethylsilyldiazomethane was quenched by acetic acid. This process was used to improve the compatibility between polymer and THF phase GPC. The PS-*b*-PMAA block copolymers were converted to PS-*b*-PMMA to prevent self-assembly of PS-*b*-PMAA in THF due to the incompatibly between PMAA and THF solvent.

3.6. Characterization

^{1}H NMR (Bruker ARX 300/ARX 400) was conducted using CD_3OD as the solvent. Molecular weights and dispersity were determined using a GPC with a 515 high pressure liquid chromatography (HPLC) pump, a 2410 refractive index detector, and three Styragel columns. The columns consist of HR1, HR3, and HR4 in the effective molecular weight ranges of 100–5000, 500–30 000, and 5000–500 000, respectively. THF was used as eluent at 30 °C and flow rate was adjusted to 1.0 mL min^{-1}. Molecular weights were calibrated with poly(methyl methacrylate) standards obtained from Polymer Laboratories. Dynamic light scattering characterizations were conducted using Zetasizer Nano ZS90 from Malvern. Infrared spectra were obtained using a BioRad Excalibur FTS3000 spectrometer. The TEM was performed on a Hitachi H8000 TEM at an accelerating voltage of 200 kV. The samples were prepared by depositing a drop of the diluted nanoparticle solution in methanol on copper grids. Scanning electron microscopy was performed by drop-casting 10 µL of diluted nanoparticle solution on copper grids with carbon film.

3.7. GPC Deconvolution Analysis

The GPC deconvolution analysis using Gaussian function was used to quantify blocking efficiency. GPC traces were split into three peaks: the block copolymer, the "unreacted" homopolymer PS, and PS homopolyer by coupling. The different dn/dc values for each component were taken into account when integrating the area of each peak. Since the PMAA block was converted to PMMA prior to GPC analysis, the dn/dc value of 0.086 for PMMA and 0.186 for PSt in THF was used for calculation of the dn/dc values of the block copolymer together with weight fraction of the two blocks (w_{p1}, w_{p2}) calculated from ^{1}H NMR

$$\left(\frac{dn}{dc}\right)_{BCP} = w_{p_1}\left(\frac{dn}{dc}\right)_{p_1} + w_{p_2}\left(\frac{dn}{dc}\right)_{p_2} \tag{1}$$

To estimate the mole fraction of each peak, the areas of the peaks were obtained via Origin Peak Analyzer and normalized with respect to molecular weight and dn/dc

$$x_1 = \frac{\dfrac{A_1}{\left(\dfrac{dn}{dc}\right)_1 * M_1}}{\dfrac{A_1}{\left(\dfrac{dn}{dc}\right)_1 * M_1} + \dfrac{A_2}{\left(\dfrac{dn}{dc}\right)_2 * M_2} + \dfrac{A_3}{\left(\dfrac{dn}{dc}\right)_3 * M_3}} \tag{2}$$

$$x_2 = \frac{\dfrac{A_2}{\left(\dfrac{dn}{dc}\right)_2 * M_2}}{\dfrac{A_1}{\left(\dfrac{dn}{dc}\right)_1 * M_1} + \dfrac{A_2}{\left(\dfrac{dn}{dc}\right)_2 * M_2} + \dfrac{A_3}{\left(\dfrac{dn}{dc}\right)_3 * M_3}} \tag{3}$$

$$x_3 = \frac{\dfrac{A_3}{\left(\dfrac{dn}{dc}\right)_3 * M_3}}{\dfrac{A_1}{\left(\dfrac{dn}{dc}\right)_1 * M_1} + \dfrac{A_2}{\left(\dfrac{dn}{dc}\right)_2 * M_2} + \dfrac{A_3}{\left(\dfrac{dn}{dc}\right)_3 * M_3}} \tag{4}$$

Reproducibility was ensured with five deconvolutions to obtain an average and standard deviation within 2%. This

© 2017 WILEY-VCH Verlag GmbH & Co. KGaA, Weinheim

method follows the procedure established by Bartels et al. and Jennings et al.[11,12]

4. Conclusions

A reversed monomer addition sequence was successfully utilized to prepare bimodal polymer grafted nanoparticles and resulted in a significantly condensed synthetic procedure. The composition of the grafted polymers was analyzed by GPC deconvolution. Approximately 10% of the grafted PS macroinitiators were chain extended while the majority remained "unreacted" or were terminated by radical coupling. It was shown that this procedure of grafting block polymers with reversed monomer addition sequence could be employed as a "quick and dirty" method of preparing mixed brush polymer grafted nanoparticles. The SiO_2-*g*-(PS_{396}, PS_{396}-*b*-$PMAA_x$) nanoparticles showed unique self-assembly behavior and formed solid spherical aggregates. The degree of aggregation could be controlled in the range between one and several hundred by adjusting the PS/PMAA ratio and initial nanoparticle concentration. It is expected that these assemblies will find wide application in the nanotechnology field.

Supporting Information

Supporting Information is available from the Wiley Online Library or from the author.

Acknowledgements

B.C.B. acknowledges financial support from the South Carolina SmartState Centers of Economic Excellence program.

Conflict of Interest

The authors declare no conflict of interest.

Keywords

diblock copolymers, nanocomposites, nanoparticles, polystyrene (PS), reversible addition fragmentation chain transfer

Received: May 10, 2017
Revised: July 12, 2017
Published online: August 14, 2017

[1] D. J. Keddie, *Chem. Soc. Rev.* **2014**, *43*, 496.
[2] K. Matyjaszewski, *Macromolecules* **2012**, *45*, 4015.
[3] C. Tang, T. Kowalewski, K. Matyjaszewski, *Macromolecules* **2003**, *36*, 1465.
[4] Y. Qiao, X. Yin, L. Wang, M. S. Islam, B. C. Benicewicz, H. J. Ploehn, C. Tang, *Macromolecules* **2015**, *48*, 8998.
[5] Y. Li, P. Tao, A. Viswanath, B. C. Benicewicz, L. S. Schadler, *Langmuir* **2013**, *29*, 1211.
[6] A. Rungta, B. Natarajan, T. Neely, D. Dukes, L. S. Schadler, B. C. Benicewicz, *Macromolecules* **2012**, *45*, 9303.
[7] B. Zhao, L. Zhu, *Macromolecules* **2009**, *42*, 9369.
[8] J. Yan, T. Kristufek, M. Schmitt, Z. Wang, G. Xie, A. Dang, C. M. Hui, J. Pietrasik, M. R. Bockstaller, K. Matyjaszewski, *Macromolecules* **2015**, *48*, 8208.
[9] Y. Zheng, Y. Huang, Z. M. Abbas, B. C. Benicewicz, *Polym. Chem.* **2016**, *7*, 5347.
[10] Y. Zheng, Y. Huang, Z. M. Abbas, B. C. Benicewicz, *Polym Chem.* **2017**, *8*, 370.
[11] J. W. Bartels, S. I. Cauët, P. L. Billings, L. Y. Lin, J. Zhu, C. Fidge, D. J. Pochan, K. L. Wooley, *Macromolecules* **2010**, *43*, 7128.
[12] J. Jennings, M. Beija, J. T. Kennon, H. Willcock, R. K. O'Reilly, S. Rimmer, S. M. Howdle, *Macromolecules* **2013**, *46*, 6843.

 © 2017 WILEY-VCH Verlag GmbH & Co. KGaA, Weinheim